

Sanguinarine is reduced by NADH through a covalent adduct



Roman Sandor ^a, Jiri Slanina ^a, Adam Midlik ^{b, c}, Kristyna Sebrlova ^a, Lucie Novotna ^a,
Martina Carnecka ^a, Iva Slaninova ^d, Petr Taborsky ^e, Eva Taborska ^a, Ondrej Pes ^{a, *}

^a Department of Biochemistry, Faculty of Medicine, Masaryk University, Kamenice 5, 62500 Brno, Czech Republic

^b National Centre for Biomolecular Research, Faculty of Science, Masaryk University Brno, Kamenice 5, 62500 Brno, Czech Republic

^c Central European Institute of Technology CEITEC MU, Kamenice 5, 62500 Brno, Czech Republic

^d Department of Biology, Faculty of Medicine, Masaryk University, Kamenice 5, 62500 Brno, Czech Republic

^e Department of Chemistry, Faculty of Science, Masaryk University, Kamenice 5, 62500 Brno, Czech Republic

ARTICLE INFO

Article history:

Received 21 April 2017

Received in revised form

26 October 2017

Accepted 27 October 2017

Keywords:

Benzophenanthridine alkaloids

Ene adduct

Hydride transfer

LC-MS

NADH

NADH depletion

Redox cycling

Sanguinarine

ABSTRACT

Sanguinarine is a benzo[c]phenanthridine alkaloid with interesting cytotoxic properties, such as induction of oxidative DNA damage and very rapid apoptosis, which is not mediated by p53-dependent signaling. It has been previously documented that sanguinarine is reduced with NADH even in absence of any enzymes while being converted to its dihydro form. We found that the dark blue fluorescent species, observed during sanguinarine reduction with NADH and misinterpreted by Matkar et al. (Arch. Biochem. Biophys. 2008, 477, 43–52) as an anionic form of the alkaloid, is a covalent adduct formed by the interaction of NADH and sanguinarine. The covalent adduct is then converted slowly to the products, dihydrosanguinarine and NAD⁺, in the second step of reduction. The product of the reduction, dihydrosanguinarine, was continually re-oxidized by the atmospheric oxygen back to sanguinarine, resulting in further reacting with NADH and eventually depleting all NADH molecules. The ability of sanguinarine to diminish the pool of NADH and NADPH is further considered when explaining the sanguinarine-induced apoptosis in living cells.

© 2017 Elsevier Ltd. All rights reserved.

1. Introduction

Sanguinarine (SA) belongs to a family of plant secondary metabolites called quaternary benzo[c]phenanthridine alkaloids (QBAs). These compounds have been extensively studied for their numerous biological activities, such as antitumor, antimicrobial, antifungal, and anti-inflammatory. While the results have been summarized in several works, the greatest attention is given to the anticancer activity of QBAs (Slaninova et al., 2014; Gaziano et al., 2016). It has been reported that SA is *in vitro* cytotoxic preferentially toward cancer cells than normal cells at concentrations that are comparable to those of the current clinically used anticancer agents (Ahmad et al., 2000). Under physiological conditions, a hydroxide anion (OH⁻) is reversibly attached to the iminium bond of SA to give a 6-hydroxy product called an alkanolamine or a pseudo-base (Fig. 1). The alkanolamine form, which is a nonpolar uncharged molecule, can easily enter a cell to establish a new, pH-

dependent equilibrium between the iminium and alkanolamine form inside the cell. The alkaloid toxicity depends on the ability of the planar, charged quaternary form of SA to produce a stable complex with DNA, which subsequently could affect the cell viability (Slaninova et al., 2001; Vacek et al., 2011). Treatment of cells with SA led to a rapid production of reactive oxygen species (ROS) (Burgeiro et al., 2013), fast and severe glutathione depletion (Debiton et al., 2003), oxidative DNA damage and very rapid apoptosis that was not mediated by p53-dependent DNA damage signaling (Matkar et al., 2008a; Hammerova et al., 2011). The first step in the metabolism of SA in rat liver is the reduction of the quaternary form to dihydrosanguinarine (DHSA) (Fig. 1). The conversion might be mediated by several NAD(P)H dependent oxidoreductases (Deroussent et al., 2010; Wu et al., 2013). In cell cultures of *Eschscholzia californica*, SA is reabsorbed and reduced to DHSA by sanguinarine reductase, which was isolated (Weiss et al., 2006) and characterized (Vogel et al., 2010). Additionally, it has been observed that SA underwent the conversion to its inactive reduced form even when incubated with NADH in the absence of any enzyme (Kovar et al., 1986; Matkar et al., 2008b), however; physiologically important reducing agents, such as glutathione and L-ascorbic acid,

* Corresponding author.

E-mail address: ondramayl@gmail.com (O. Pes).

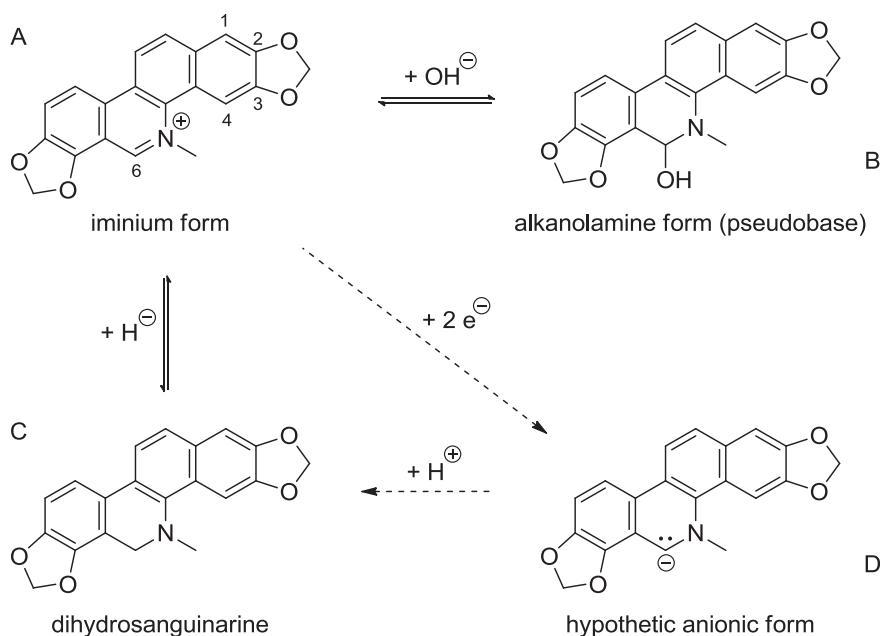


Fig. 1. A molecule of sanguinarine in A) an iminium (a quaternary) form, B) an alkanolamine form, C) dihydrosanguinarine, and D) a hypothetic anionic form suggested by Matkar et al. (2008b). The iminium form exhibits yellow fluorescence while the forms B and C glow dark blue under the UV light.

were unable to effectively reduce SA (Kosina et al., 2011). On top of that, SA, as well as other QBAs, may undergo a complex series of metabolic changes, some of which may contribute to their biological effects (Sandor et al., 2016).

When studying a relationship between the cell death and the ability of SA to deplete the cellular antioxidant capacity Matkar et al. (2008b) observed a novel, dark blue fluorescent, anionic form of SA formed by the reduction with NADH in the absence of any enzyme. The authors detected a new form of SA by reversed phase thin layer chromatography (RP-TLC) and determined the negative charge of species by gel electrophoresis. While a new form of SA would be somewhat fascinating, an alternative explanation of these findings could be presented and interpreted.

In this study, we have employed chromatographic and spectrometric techniques to give a novel interpretation of SA being reduced with NADH to DHSA. We found that the dark blue fluorescent anion produced during SA reduction with NADH, originally observed by Matkar et al. (2008b), is a covalent adduct formed by the reaction of NADH and SA. The adduct is then converted slowly to products, DHSA and NAD⁺, in the second step of reduction. DHSA is continuously re-oxidized back to SA by the atmospheric oxygen resulting in eventual NADH depletion.

2. Results

2.1. Reduction of SA with NADH forms an unexpected spot on thin-layer chromatography

First, we have aimed to reproduce the RP-TLC performed by Matkar et al. (2008b). Resulting chromatograms might be seen in Fig. 2. The retention factor (*R_f*) for NADH was one as it traveled along with the polar mobile phase with no retention on the non-polar solid phase. Visualization under UV light (340 nm) showed a fluorescence band of NADH broadened over the entire chromatogram concentrating at the head. The same band at the head of the chromatogram was clearly visible in the line where NADH was mixed with SA. This was in accordance with our expectations as the NADH molecule was negatively charged and thus highly polar. Dark

blue fluorescence was clearly visible in the lines where SA was mixed with NADH (*R_f* ~ 0.75) and with NaBH₄ (*R_f* ~ 0.35). After four hours in dark, both dark blue spots turned their fluorescence to the same orange-yellow color as it has been observed in the sole SA line (Fig. 2B). A lower *R_f* of the dark blue spot in the SA + NaBH₄ line allowed for identification as DHSA as it was characterized by blue fluorescence and a decrease in polarity, which had resulted from a loss of the charged quaternary form. The same DHSA band would have been observed in the SA + NADH line if the mixture had been applied onto a TLC plate after a longer time (data not shown). A spot between SA and DHSA (*R_f* ~ 0.45) observed at lines of pure SA and SA + NADH probably represented an alkanolamine form of SA. Another dark blue fluorescent spot in the SA + NADH line with *R_f* ~ 0.75 could not have been attributed to any known species of SA and was then studied comprehensively by liquid chromatography with mass spectrometric detection (LC-MS).

2.2. Sanguinarine forms a covalent adduct with NADH

LC-MS was employed as a next step in revealing the origin of the interaction between SA and the NADH molecule. A representative chromatogram of an LC-MS method at very similar conditions to those used for RP-TLC might be seen in Fig. 3. The product, formed from the reaction between SA and NADH, was then expected to elute around the tenth minute. Detection at 280 nm and by MS showed a few distinct peaks around that retention time. In order to be able to identify the product, positive mode MS and MS/MS spectra were acquired (Fig. 4). Peaks observed in Fig. 4 might be accordingly assigned to the pure reactants (SA at 332 Da and NADH at 666 Da) as well as to the product of their reaction (997 Da for a singly charged and 499 Da for a doubly charged ion). The MS/MS spectrum of the doubly charged ion produces only SA as a major fragment. This fragmentation might be explained by a favorable formation of an aromatic quaternary form of SA and a neutral residue of NADH. In other words, SA is a good leaving fragment while retaining its charge as it contains quaternary nitrogen. In negative mode, the adduct was observed at 995 Da (data not shown) indicating that the mass of the neutral species was 996 Da.

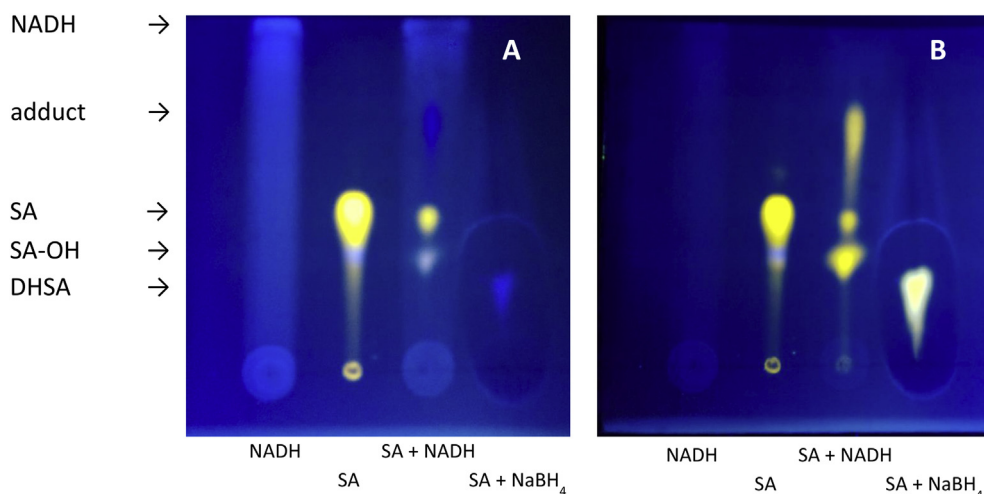


Fig. 2. RP-TLC of NADH, SA, an equimolar mixture SA + NADH, and a mixture of SA with NaBH₄ after A) 15 min, B) 240 min. SA-OH – an alkanolamine form of SA. For details, please see text.

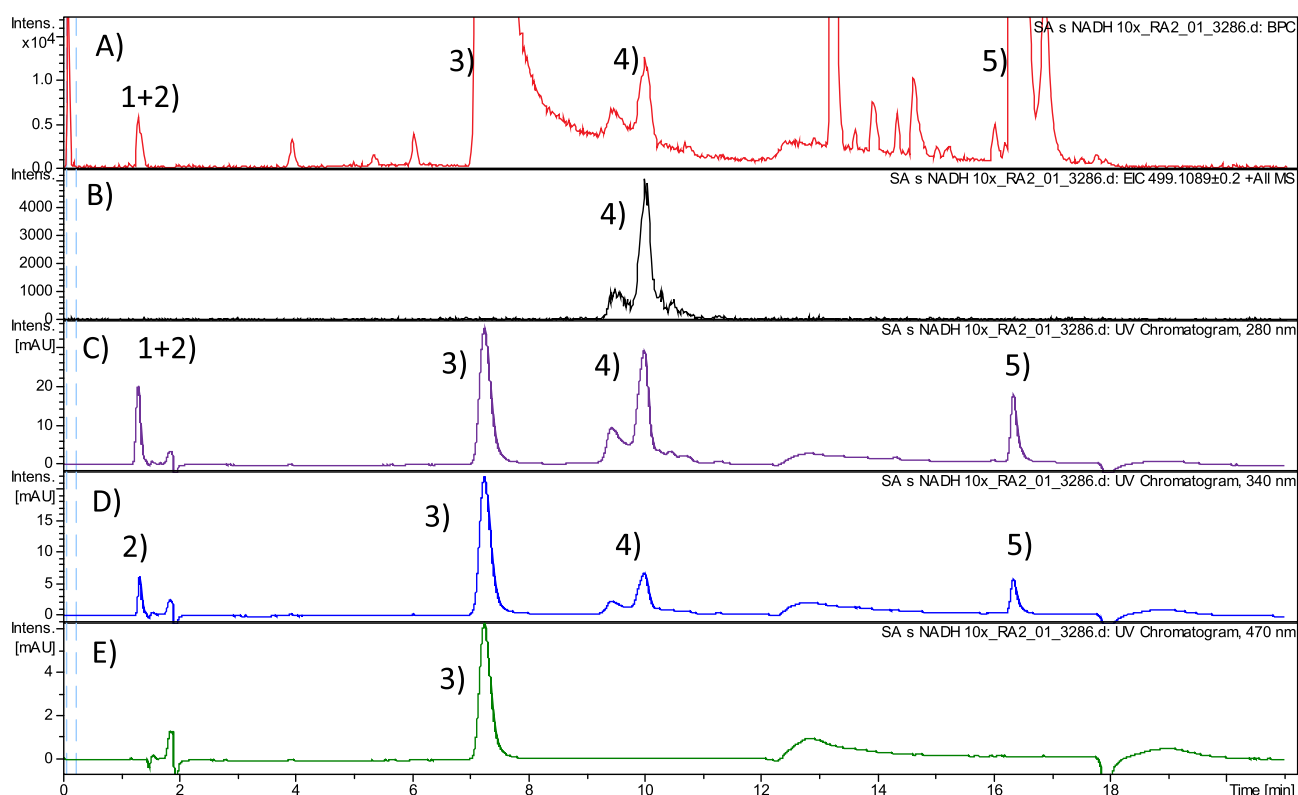


Fig. 3. Liquid chromatography of SA mixed with NADH after 2 h of reaction with detection A) MS of a base peak, B) MS of an extracted ion m/z 499.1089 ± 0.2 C) at 280 nm, D) at 340 nm, E) at 470 nm. Peaks are labeled as follows: 1) NAD⁺, 2) NADH, 3) SA, 4) a group of adducts of SA with NADH, 5) DHSA. SA is the only colorful compound as it absorbs visible light. For details, please see text. (For interpretation of the references to colour in this figure legend, the reader is referred to the web version of this article.)

To confirm that the 997 Da ion is a covalent adduct and not just an association of SA and NADH (332 Da + 665 Da = 997 Da) in a liquid or gas phase, the diode-array spectra of the substrates and products were evaluated, see Fig. 5. All chromatographic peaks of the adduct absorbed at 280 and 340 nm which were also the absorption maxima of NADH. However, the characteristic absorption maximum of the SA quaternary form (470 nm) was not found in the peaks of the adducts. Since the formation of the adduct led to discoloration of SA, the 997 Da adduct should not be considered a mass spectrometry gas phase species and a covalent bond was

likely to be formed. The existence of more than one peak around the 10th minute evoked the product existed in several isomeric forms; please see Discussion for more details.

The adduct is likely to be the same substance observed by Matkar et al. (2008b) in their experiments due to the similar properties (such as negative charge, polarity, and dark-blue fluorescence changing with time). At neutral pH, the net charge of the adduct is (−1), because the negative charge of phosphate groups (−2) is only partially weakened by the positively charged nitrogen atom of pyridine (+1). The net negative charge of the product was

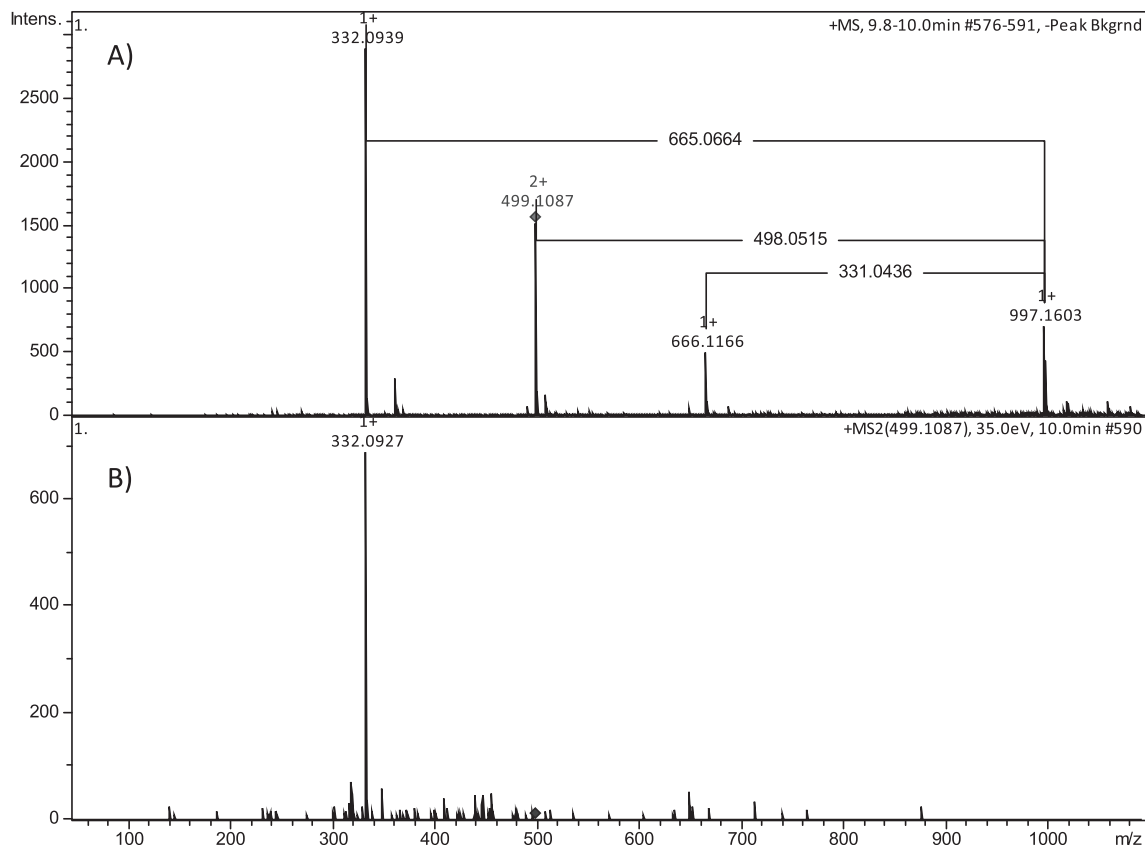


Fig. 4. A positive ESI A) MS spectrum of the SA + NADH adduct from the 10th min (Fig. 3) and B) MS/MS spectrum of the doubly charged, monoisotopic adduct ion 499.1087 Da (theoretical 499.1119 Da). Other monoisotopic signals belong to a singly charged adduct 997.1603 Da (theoretical 997.2165 Da), an ion of NADH 666.1166 Da (theoretical 666.1320 Da), and an ion of SA 332.0939 Da (theoretical 332.0917 Da).

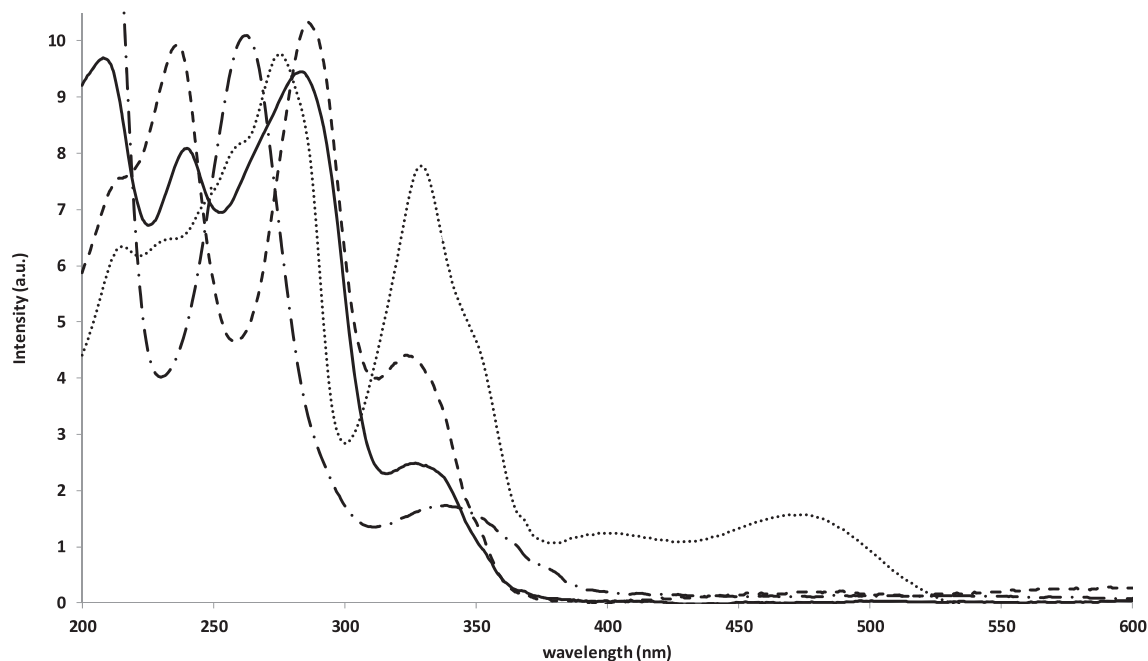


Fig. 5. Diode-array spectrum of the NADH-SA adduct (solid), NAD⁺/NADH (dash-dotted) SA (dotted), and DHSA (dashed). The spectra have been normalized to the adduct maximum intensity at 280 nm.

originally incorrectly interpreted as a new form of SA, which was not supported by any evidence (Matkar et al., 2008b). Furthermore, if the anionic species had truly existed, it should have been a highly

unstable, as it would have immediately accepted a proton from water (Fig. 1).

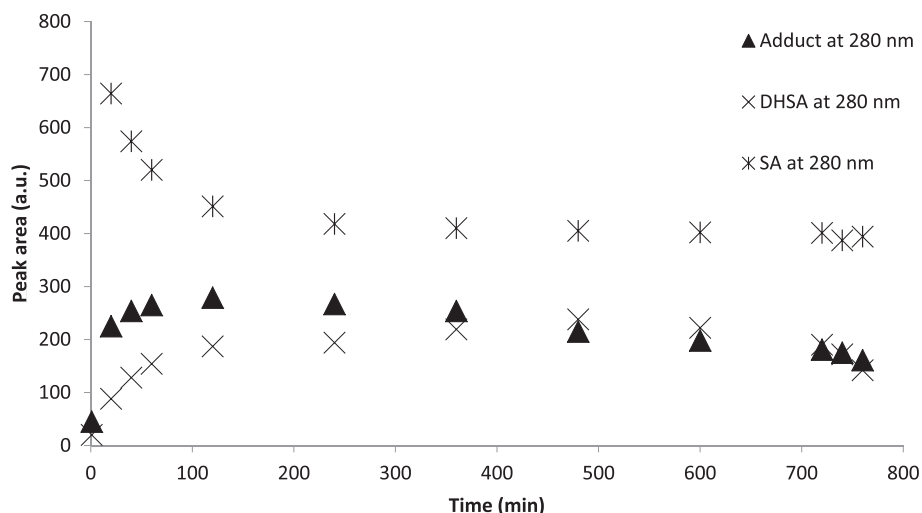


Fig. 6. NADH and SA were mixed as described in section 5.3, sealed under Ar and twelve consecutive LC-MS runs were performed. The initial rates expressed as a slope of a linear regression from the first three points were -11.0 , $+5.3$, and $+2.8$ peak area/minute for SA, the adduct, and DHSA respectively.

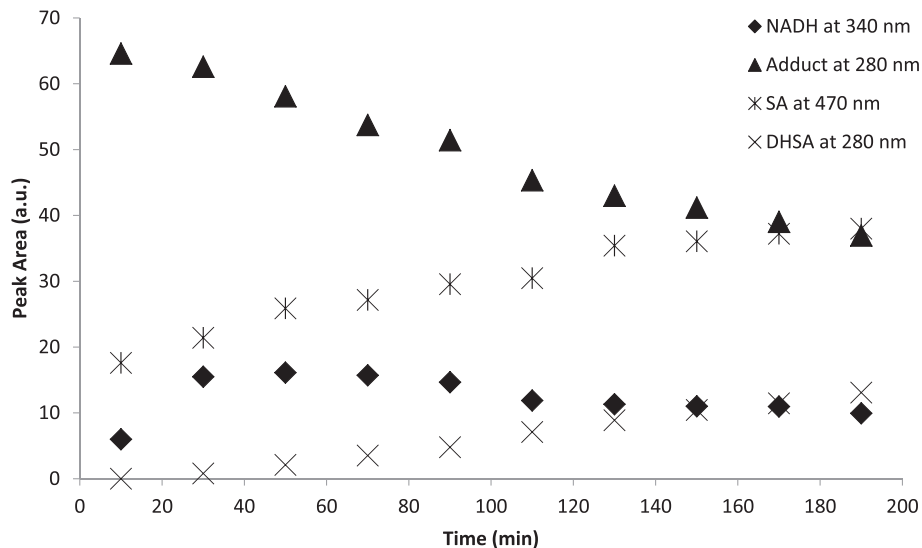


Fig. 7. Ten consecutive LC-MS runs from a vial with the adduct transferred from the fraction collected by semi-preparative chromatography. NADH peak area is kept at a constant level while the peak area of DHSA increases.

2.3. The covalent adduct is an intermediate in the reduction of SA with NADH

Kinetics of the reaction was measured to explore if the covalent adduct was involved in the final reduction of SA to DHSA. It is worth noting, that the same reduction reaction was described by Kovar et al. (1986); however, the authors did not attempt to clarify the mechanism of the reduction, although they suggested a rather complex transition state, which must have been formed between the target molecules. The formation kinetics at 280 nm might be seen in Fig. 6, which clearly showed an increased concentration of the adduct and DHSA over time. While the maximum concentration of the adduct was observed in 120 min, DHSA reached its peak concentration in about 480 min. In other words, the higher rate of the adduct formation than the rate of its decomposition to DHSA suggested that the adduct was truly necessary for the reaction to be completed. The decline in SA concentration was biphasic with the fast decrease occurring in the first 120 min followed by a slow

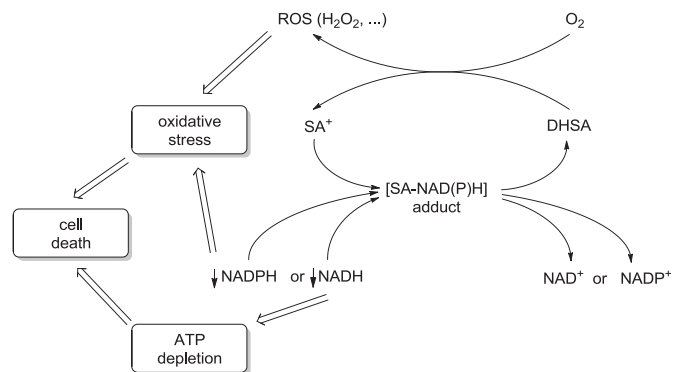


Fig. 8. Representation of the NAD(P)H depletion effect caused by continual re-oxidation of DHSA. SA⁺ - a quaternary form, SA-NAD(P)H - the adduct of SA⁺ with NADH.

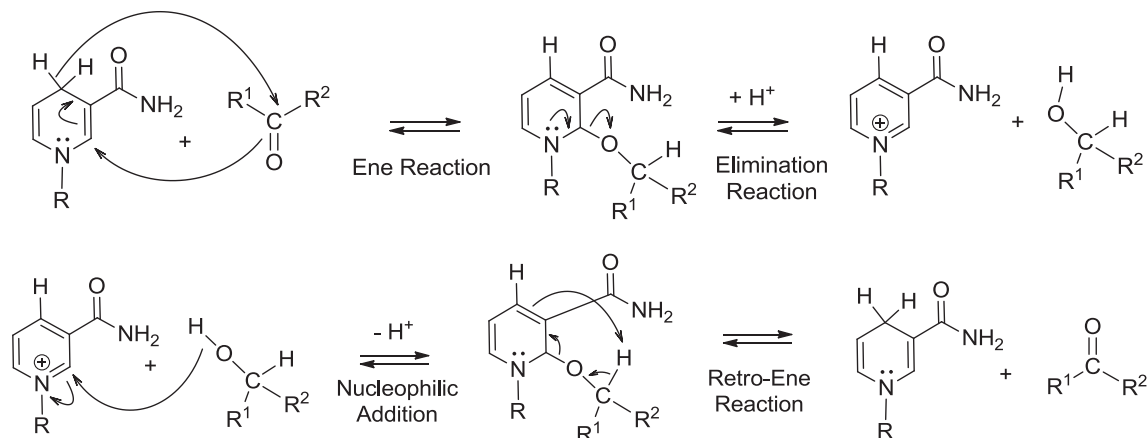


Fig. 9. The proposed Ene mechanism for NADH dehydrogenases, the upper figure shows NADH oxidation, the lower figure shows NAD⁺ reduction, according to [Hamilton \(1971\)](#); [Libby and Mehl \(2012\)](#).

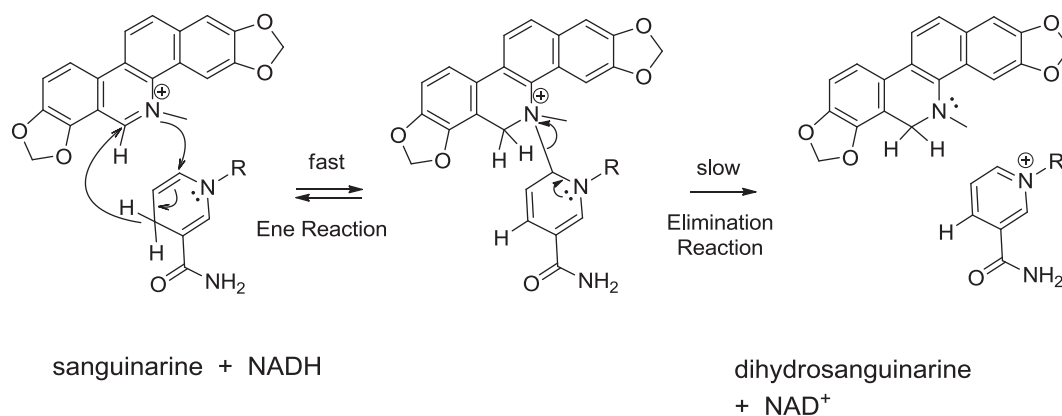


Fig. 10. Reduction of SA with NADH based on the proposed Ene adduct mechanism.

decrease. It corresponds to the rapid formation and a slow decomposition of the adduct. The additional decrease in DHS after the 480th minute is caused by re-oxidation of the entire mixture by the atmospheric oxygen. If the vials had not been sealed under argon atmosphere, the re-oxidation would have appeared around the 400th minute and the resulting DHS would have been subsequently converted to SA (data not shown).

In order to support our hypothesis that the adduct was a real intermediate in the reduction of SA with NADH, the adduct has been isolated by semi-preparative LC and its further conversion was immediately analyzed by LC-UV-MS, as seen in [Fig. 7](#). Initially, the adduct was partially converted back to reactants, SA and NADH, indicating that the formation of the covalent adduct was reversible. The NADH concentration had peaked around 50 min and then declined very slowly. This decrease in NADH concentration indicated the presence of additional reaction. At the same time, the concentration of the adduct and DHS kept decreasing and slowly increasing, respectively. This suggested that the additional reaction was the conversion of the adduct to DHS and that the adduct was indeed a true intermediate of the reaction. The continuous increase in the SA concentration could be explained as a sum of a velocity of the initial reversed reaction and a velocity of DHS oxidation caused by the atmospheric oxygen.

It is worth to note that the equilibrium conditions in the vial from the fraction collector were substantially different from those when the mixture was fresh. When SA and NADH were freshly mixed the excess of NADH made sure the reaction would progress,

up to some point, in a reducing environment. On the other hand, when a fraction containing the adduct was removed from the collector and transferred to the LC-MS vial, the equilibrium was shifted to the left *i.e.*, the adduct partially decomposed to reactants (NADH and SA) and a part was converted to products (NAD⁺ and DHS).

When the reaction was left overnight to proceed completely, SA and NAD⁺ were the only compounds observed in the reaction mixture. SA catalyzed the oxidation of NADH by the air oxygen, in other words, sanguinarine showed an oxygen-NADH oxidoreductase-like activity. This effect of SA is probably the reason why SA and other QBAs could deplete NAD(P)H in the cells and induce rapid cell death ([Fig. 8](#)).

3. Discussion

3.1. NADH is oxidized by SA in a two-step process involving the covalent adduct formation

In our study, we observed a formation of a covalent adduct during the reduction of SA with NADH. Although we have observed the formation of several isomeric adducts between SA and NADH with similar chromatographic properties, we expect solely a single species was converted to the products – DHS and NAD⁺.

The existence of the covalent intermediate as a result of an attack of NADH to the reactive iminium bond of SA is supported by two facts:

- 1) The molecular mass of the adduct and its respective fragmentation to SA and NADH.
- 2) Discoloration (a lack of 470 nm absorption band) and dark blue fluorescence of the adduct.

The originally postulated one-step hydride transfer to NAD⁺ has been still a prevailing mechanism of enzymatic NAD⁺ reduction especially due to an inability to detect any reaction intermediates. Here, we try to suggest another option to explain the net hydride transfer.

Hamilton (1971) proposed the formation of the covalent intermediate between an alcohol substrate and a pyridine coenzyme during oxidation catalyzed by dehydrogenases (Fig. 9, the lower panel). The first step was an electrocyclic Ene reaction, which was facilitated by transition states with aromatic character. In the second step, the adduct was decomposed to the products by an elimination reaction triggered by a proton. The Ene mechanism for hydride transfer did not receive much attention especially due to an inability to detect any reaction intermediates. Libby and Mehl (2012) found covalent Ene adduct intermediates in a dihydropyridine model for NADH reduction reactions and Rosenthal et al. (2014) detected a covalent Ene adduct intermediate in an enzymatic hydride transfer from NADPH to the corresponding substrate. The results suggested that Ene reaction mechanism could be shared by more NAD(P)H dehydrogenases.

Since we have not characterized the exact structure of the adduct, the mechanism of the SA reduction discussed here is only tentative. One possibility suggests that the reduction of SA with NADH should proceed via the Ene reaction mechanism, which is in line with previous reports (Libby and Mehl, 2012; Rosenthal et al., 2014), and the proposed reaction is given in Fig. 10. The net hydride transfer then involves transition states with aromatic character, as well as lowering activation energy.

The existence of several isomeric forms of the adduct observed in the LC chromatogram around the 10th minute (Fig. 3B) might be explained by a creation of two new adjacent stereogenic centers in the molecule of the Ene adduct – the quaternary nitrogen of SA and C-6 of the nicotinamide ring (Fig. 10). The Ene adduct then comprises two pairs of enantiomers providing two peaks on the chromatogram monitored at *m/z* 499. If we take into account the possibility of using C-2 instead of C-6 for the formation of the Ene adduct, we could obtain even four enantiomeric pairs. Such explanation is in accordance with the previous findings (Libby and Mehl, 2012), where the isomers of Ene adducts formed between a model molecule of NADH and the substrates. Both SA and NAD⁺ in the oxidized form have a pyridinium ring containing a reactive iminium bond, which plays a key role in the covalent adduct formation in the proposed Ene reaction. Considering a substrate oxidation with NAD⁺ (Fig. 9, the lower panel), the iminium bond of NAD⁺ is attacked by a nucleophilic oxygen of a hydroxylic group. Correspondingly, during the SA reduction with NADH, the reactive iminium bond of SA might have been attacked by any of the nucleophilic atoms of NADH. This would also explain the reversible formation of the isomeric adducts seen in LC-MS (Fig. 3).

4. Conclusions

In this work, we observed a novel species of a covalent adduct, which was capable of acting as an intermediate in the facilitation of the SA reduction by NADH. The idea of such an intermediate existence was postulated by Kovar et al. (1986); nevertheless, there have been no later attempts to characterize the intermediate. The species is likely to be the same molecule Matkar et al. (2008b) observed in their experiments; however, they misinterpreted the intermediate as a negatively charged species of SA.

We have shown that the process of reduction went through a stable covalent intermediate, which is contradictory to the accepted model of a one-step hydride transfer. Our data supported the covalent intermediate hypothesis, but we managed to form such an intermediate with a native molecule of NADH, instead of a hard-to-design synthetic model molecule.

The product of the reduction, DHSA, was continually re-oxidized back to SA by the atmospheric oxygen to generate a new portion of SA available for a further reaction with NADH. This fact guaranteed that the concentration of the adduct remained constant and we suppose this happens also in living cells, in which SA is quickly reduced by NAD(P)H-dependent enzymes. This idea is supported by other authors, who observed an induced apoptosis due to the rapid depletion of a reducing potential of the cell (Debiton et al., 2003; Hammerova et al., 2012; Pallichankandy et al., 2015). Inhibition of NAD(P)H-dependent enzymes by SA previously observed (Kalogris et al., 2014) could be caused by the covalent adduct due to its structural similarity with NAD(P)H.

5. Experimental

5.1. Reagents and materials

Methanol (MeOH, *p.a.*) was obtained from Penta (Czech Republic). Acetic acid (LC-MS), ammonium hydroxide (28–30% NH₃ in water), sodium formate (LC-MS), NADH disodium salt (Grade I), MeOH (LC-MS), and acetonitrile (ACN, HPLC grade, LC-MS) were purchased from Sigma–Aldrich (Czech Republic). All water used was of an ultra-pure grade supplied by an in-house Milli-Q system (Millipore, MA, USA).

5.2. Alkaloid isolation

The standards of the benzophenanthridine alkaloids originated from isolation during the systematic studies in the laboratories of the Department of Biochemistry from plant material of *Macleaya microcarpa* (Maxim.) Fedde, *Dicranostigma lactuoides* Hook. f. et Thomson, *Sanguinaria canadensis* L., and *Stylophorum lasiocarpum* (Oliv.) Fedde. Briefly, SA was prepared by extraction of dried, ground plant material with methanol in a FexIKA[®] apparatus (IKA, Germany). The extract was purified, concentrated and the last step of isolation was performed by means of semi-preparative reversed-phase (RP) chromatography. The identity of the alkaloid was verified by the LC-MS analysis.

5.3. Reaction conditions

SA was incubated with NADH in an equimolar ratio at room temperature under argon atmosphere in a sealed vial for 5 min, if not stated otherwise. For an LC-MS analysis (Fig. 6), the mixture of 0.5 ml of 1 mmol/L of alkaloid and 0.5 ml 1 mmol/L NADH was diluted ten times, sealed in an LC-MS vial under argon atmosphere, and immediately injected onto the LC-MS system. For a semi-preparative analysis, the mixture of 0.5 ml of 1 mmol/L of alkaloid and 0.5 ml of 1 mmol/L NADH was sealed under argon atmosphere, left for 60 min, and then 1 ml was injected onto the semi-preparative column specified in the section 5.4.

5.4. Adduct isolation and purification

An Agilent 1200 Series LC system (Agilent Technologies, CA, USA) equipped with a fraction collector was used for purification and isolation of the adduct. It consisted of a ternary pump, a diode array detector (DAD), a syringe loading sample injector (ECOM, Czech Republic) with a 5 ml external sample loop and a fraction

collector. The alkaloid-NADH complex was separated on a C12 column (Synergi RP-Max, 4 μm , 250 mm \times 10 mm ID, Phenomenex, CA, USA). The mobile phase consisted of ammonium formate buffer (0.05 M HCOOH titrated with NH_3 to pH = 4.50) and ACN with the following elution profile: ACN was linearly increased from 25% to 27.5% over first 5 min, then to 41.5% over the subsequent 5 min, next to 47% at the 15th minute and finally to 80% at 20 min, where it was held for 10 min before equilibration under the initial conditions for 3.0 min. The flow rate was set at 4 mL min^{-1} and fractions were collected on a peak basis using a DAD at 280 nm. Fraction identified as the adduct was transferred into an LC-MS vial and ten LC-MS runs (Fig. 7) were performed.

5.5. Liquid chromatography – mass spectrometry

The LC-MS method was developed using a Dionex Ultimate 3000RS (Thermo Scientific, CA, USA) module. Compound separation was achieved with a 3.0 mm \times 150 mm, 5 μm Synergi RP-Max C18 (Phenomenex, CA, USA) column, set at (23 \pm 0.1) $^\circ\text{C}$, and a flow-rate of 0.5 mL min^{-1} . The binary mobile phase system consisted of ammonium acetate buffer (10 mM, pH = 4.4) and ACN. After a 10- μL injection, the percentage of ACN was linearly increased from 20% to 40% over 10 min and then to 80% over the subsequent 1 min. ACN was held at 80% for 5 min, followed by equilibration under the initial conditions for another 5 min. A complete LC run was 21 min. The LC system was equipped with a DAD detector and at the same time, it was connected to a Bruker MicrOTOF-Q II (Germany) mass spectrometer operated in the positive electrospray ionization mode. The ionization conditions were determined by the software as follows: capillary voltage: 4500 V, end plate offset: –500 V, source temperature: 220 $^\circ\text{C}$, desolvation gas (nitrogen) flow: 8 L min^{-1} , nebulizer (nitrogen) pressure: 300 kPa, and collision cell voltage: 6 eV. The base peak chromatogram (BPC) was acquired in MS mode by monitoring the m/z range of 50–3000 with a spectra sample time of 1 s and MS/MS spectra were collected in a data-dependent mode. The mass spectrometer was calibrated using 10 mM sodium formate in 50% isopropyl alcohol on a daily basis and in the beginning of each LC run with a 20- μL loop flush. High-resolution MS and MS/MS spectra were first investigated to obtain the elemental formula of each compound. The final identification of target compounds relied on isotope pattern matching with a combination of MS/MS and retention behavior.

5.6. Thin-layer chromatography

Thin-layer chromatography was performed on aluminum plates (6 \times 12 cm) covered by Silica gel 18 F_{254s} (Merck, Germany) and a mobile phase consisting of ammonium formate 0.1 M and MeOH (92:8 v/v). The chamber with the mobile phase was left covered for 20 min to saturate before any separation. Samples were immediately after mixing applied to the plate, which was after drying (2–3 min) inserted into the chamber with the mobile phase. The separation took approximately ten minutes. After the experiment, the TLC plate was removed, allowed to dry for 15 min, visually inspected and photographed under UV light at 340 nm.

Acknowledgement

This work was supported by funds from the Faculty of Medicine MU to a junior researcher Ondřej Peš and by the Specific University Research Grant (MUNI/A/1205/2016, MUNI/A/1237/2016, MUNI/A/0810/2016) provided by the Ministry of Education, Youth and Sports of the Czech Republic in the year 2016.

References

- Ahmad, N., Gupta, S., Husain, M.M., Heiskanen, K.M., Mukhtar, H., 2000. Differential antiproliferative and apoptotic response of sanguinarine for cancer cells versus normal cells. *Clin. Cancer Res.* 6, 1524–1528.
- Burgeiro, A., Bento, A.C., Gajate, C., Oliveira, P.J., Mollinedo, F., 2013. Rapid human melanoma cell death induced by sanguinarine through oxidative stress. *Eur. J. Pharmacol.* 705, 109–118. <https://doi.org/10.1016/j.ejphar.2013.02.035>.
- Debiton, E., Madelmont, J.C., Legault, J., Barthelemeuf, C., 2003. Sanguinarine-induced apoptosis is associated with an early and severe cellular glutathione depletion. *Cancer Chemother. Pharmacol.* 51, 474–482.
- Deroussent, A., Re, M., Hoellinger, H., Cresteil, T., 2010. Metabolism of sanguinarine in human and in rat: characterization of oxidative metabolites produced by human CYP1A1 and CYP1A2 and rat liver microsomes using liquid chromatography-tandem mass spectrometry. *J. Pharm. Biomed. Anal.* 52, 391–397. <https://doi.org/10.1016/j.jpba.2009.09.014>.
- Gaziano, R., Moroni, G., Buè, C., Miele, M.T., Sinibaldi-Vallebona, P., Pica, F., 2016. Antitumor effects of the benzophenanthridine alkaloid sanguinarine: evidence and perspectives. *World J. Gastrointest. Oncol.* 8, 30–39. <https://doi.org/10.4251/wjgo.v8.i1.30>.
- Hamilton, G.A., 1971. Proton in biological redox reactions. *Prog. Bioorg. Chem.* 1, 83–157.
- Hammerova, J., Uldrijan, S., Taborska, E., Slaninova, I., 2011. Benzo[c]phenanthridine alkaloids exhibit strong anti-proliferative activity in malignant melanoma cells regardless of their p53 status. *J. Dermatol. Sci.* 62, 22–35. <https://doi.org/10.1016/j.jderm.2011.01.006>.
- Hammerova, J., Uldrijan, S., Taborska, E., Vaculova, A.H., Slaninova, I., 2012. Necroptosis modulated by autophagy is a predominant form of melanoma cell death induced by sanguinarine. *Biol. Chem.* 393, 647–658. <https://doi.org/10.1515/hbsz-2011-0279>.
- Kalogris, C., Garulli, C., Pietrella, L., Gambini, V., Pucciarelli, S., Lucci, C., Tilio, M., Zabaleta, M.E., Bartolacci, C., Andreani, C., Giangrossi, M., Iezzi, M., Belletti, B., Marchini, C., Amici, A., 2014. Sanguinarine suppresses basal-like breast cancer growth through dihydrofolate reductase inhibition. *Biochem. Pharmacol.* 90, 226–234. <https://doi.org/10.1016/j.bcp.2014.05.014>.
- Kosina, P., Vacek, J., Papouskova, B., Stiborova, M., Styskala, J., Cankar, P., Vrublova, E., Vostalova, J., Simanek, V., Ulrichova, J., 2011. Identification of benzo[c]phenanthridine metabolites in human hepatocytes by liquid chromatography with electrospray ion-trap and quadrupole time-of-flight mass spectrometry. *J. Chromatogr. B Anal. Technol. Biomed. Life Sci.* 879, 1077–1085. <https://doi.org/10.1016/j.jchromb.2011.03.023>.
- Kovar, J., Stejskal, J., Paulova, H., Slavik, J., 1986. Reduction of quaternary benzo-phenanthridine alkaloids by NADH and NADPH. *Collect. Czech. Chem. Commun.* 51, 2626–2634.
- Libby, R.D., Mehl, R.A., 2012. Characterization of covalent Ene adduct intermediates in “hydride equivalent” transfers in a dihydropyridine model for NADH reduction reactions. *Bioorg. Chem.* 40, 57–66. <https://doi.org/10.1016/j.bioorg.2011.10.002>.
- Matkar, S.S., Wrischnik, L.A., Hellmann-Blumberg, U., 2008a. Sanguinarine causes DNA damage and p53-independent cell death in human colon cancer cell lines. *Chem. Biol. Interact.* 172, 63–71. <https://doi.org/10.1016/j.cbi.2007.12.006>.
- Matkar, S.S., Wrischnik, L.A., Hellmann-Blumberg, U., 2008b. Production of hydrogen peroxide and redox cycling can explain how sanguinarine and chelerythrine induce rapid apoptosis. *Arch. Biochem. Biophys.* 477, 43–52. <https://doi.org/10.1016/j.abb.2008.05.019>.
- Pallichankandy, S., Rahman, A., Thayyullathil, F., Galadari, S., 2015. ROS-dependent activation of autophagy is a critical mechanism for the induction of anti-glioma effect of sanguinarine. *Free Radic. Biol. Med.* 89, 708–720. <https://doi.org/10.1016/j.freeradbiomed.2015.10.404>.
- Rosenthal, R.G., Ebert, M.O., Kiefer, P., Peter, D.M., Vorholt, J.A., Erb, T.J., 2014. Direct evidence for a covalent ene adduct intermediate in NAD(P)H-dependent enzymes. *Nat. Chem.* 10, 50–55. <https://doi.org/10.1038/NCHEM.1385>.
- Sandor, R., Midlik, A., Sebrlova, K., Dovrtelova, G., Noskova, K., Jurica, J., Slaninova, I., Taborska, E., Pes, O., 2016. Identification of metabolites of selected benzophenanthridine alkaloids and their toxicity evaluation. *J. Pharm. Biomed. Anal.* 121, 174–180. <https://doi.org/10.1016/j.jpba.2016.01.024>.
- Slaninova, I., Taborska, E., Bochorakova, H., Slanina, J., 2001. Interaction of benzo[c]phenanthridine and protoberberine alkaloids with animal and yeast cells. *Cell Biol. Toxicol.* 17, 51–63. <https://doi.org/10.1023/A:1010907231602>.
- Slaninova, I., Pencikova, K., Urbanova, J., Slanina, J., Taborska, E., 2014. Antitumour activities of sanguinarine and related alkaloids. *Phytochem. Rev.* 13, 51–68. <https://doi.org/10.1007/s11101-013-9290-8>.
- Vacek, J., Vrublova, E., Kubala, M., Janovska, M., Fojta, M., Simkova, E., Styskala, J., Skopalova, J., Hrbac, J., Ulrichova, J., 2011. Oxidation of sanguinarine and its dihydro-derivative at a pyrolytic graphite electrode using ex situ voltammetry. Study of the interactions of the alkaloids with DNA. *Electroanalysis* 23, 1671–1680. <https://doi.org/10.1002/elan.201100028>.
- Vogel, M., Lawson, M., Sippl, W., Conrad, U., Roos, W., 2010. Structure and mechanism of sanguinarine reductase, an enzyme of alkaloid detoxification. *J. Biol. Chem.* 285, 18397–18406. <https://doi.org/10.1074/jbc.M109.088989>.
- Weiss, D., Baumerkt, A., Vogel, M., Roos, W., 2006. Sanguinarine reductase, a key enzyme of benzophenanthridine detoxification. *Plant, Cell & Environ.* 29, 291–302. <https://doi.org/10.1111/j.1365-3040.2005.01421.x>.
- Wu, Y., Liu, Z.Y., Cao, Y., Chen, X.J., Zeng, J.G., Sun, Z.L., 2013. Reductive metabolism of the sanguinarine iminium bond by rat liver preparations. *Pharmacol. Rep.* 65, 1391–1400.